Received: 11 March 2020 | Revised: 29 July 2020 | Accepted: 27 August 2020
DOI: 10.1002/aoc.6017

FULL PAPER

Applied Organometallic Chemistry WILEY

# Copper(II) complex intercalated graphene oxide nanocomposites as versatile, reusable catalysts for click reaction

**Angel Green Samuel**[1] | **Karthikeyan Nagarajan**[1,4] | **Karthick Cidhuraj**[1] | **Bhalerao Gopal**[2] | **Sujay Chakravarty**[2] | **Varadharajaperumal Selvaraj**[3] | **Emmanuvel Lourdusamy**[1] | **Jebasingh Bhagavathsingh**[1]

[1]Department of Chemistry, Karunya Institute of Technology and Sciences, Coimbatore, Tamilnadu, India

[2]Material Characterization Division, UGC-DAE-Consortium for Research, IGCAR-Kalpakkam Node, Kalpakkam, Chennai, India

[3]Centre for Nanoscience and Engineering (CeNSE), Indian Institute of Science, Bengaluru, India

[4]Quality Control Lab, GVK Biosciences Pvt. Ltd., Jigani, Karnataka, India

**Correspondence**
Jebasingh Bhagavathsingh, Department of Chemistry, Karunya Institute of Technology and Sciences, Coimbatore 641114. Tamilnadu, India.
Email: jebasinghb@karunya.edu

**Funding information**
UGC DAE Consortium Scientific Research, IGCAR-Kalpakkam, Grant/Award Number: CSR/Acctts/2016-17/1347; Department of Science and Technology, DST-DPRP, Grant/Award Number: VI-D&P/562/2016-17/TDT(C)

In this work, we report the efficient, high stable copper(II) complexes intercalated graphene oxide (GO) used as green catalysts for copper(II) complex mediated click reaction. Copper(II) *Bis*(2,2′-bipyridine) [$Cu^{II}$ $(bpy)_2$] (C1) and Copper(II) *Bis*(1,10-phenanthroline) [$Cu^{II}$ $(phen)_2$] (C2) have synthesized for the intercalation of corresponding nanocomposites with GO, [GO@$Cu^{II}$ $(bpy)_2$] (GO-C1) and [GO@$Cu^{II}$ $(phen)_2$] (GO-C2). The noncovalent interaction of complexes supported on the surface of the GO nanosheets proves as an evident active site to facilitate the enhanced catalytic activity of copper-catalyzed alkyne azide cycloaddition ($Cu^{II}$AAC) reaction for the isolation of 1,4-disubstituted-1,2,3-triazoles as click products in shorter reaction time with 80%–91% yield (five examples). The X-ray diffraction (XRD) pattern of these composites shows the enhanced interlayers *d*-spacing range of 1.01–1.12 nm due to the intercalation of copper(II) complexes in between the GO basal planes and characterized by X-ray photoelectron spectroscopy (XPS), Fourier-transform infrared spectroscopy (FT-IR), Raman, UV, scanning electron microscope (SEM), and thermogravimetric analysis (TGA). The as-prepared nanocomposites were employed for the typical click reactions using the substrates of azide and acetylene. These classes of composite materials can be referred to recyclable, heterogeneous, green catalysts with high atom economy and could also be used for the isolation of click products in biomolecules.

KEYWORDS
1,2,3-triazoles, bipyridine ligands, click catalyst, Cu(II) complexes, intercalated graphene oxide

## 1 | INTRODUCTION

Over a few decades, among the various allotropes of carbon, graphene oxide (GO) has emerged as one of the most encouraging material because of its marvelous electronic, optical, thermal, and mechanical properties.[1–5] Due to its myriad properties, GO has also been incorporated in sustainable developments with process of green technologies[6,7] and clean energy materials.[8,9] GO is a two-dimensional carbon network with single-atom-thick lattice of honeycomb-like $sp^2$- and $sp^3$-bonded carbon atoms, bearing oxygen-containing functional groups (i.e., —OH, —C—O—C-epoxide, terminal COOH) on the surface, which are able to enhance the electron transfer rate, water dispersibility, and biocompatibility.[10–14] The presence of various functional groups in the basal and edge planes of the GO make it an ideal support for surface-engineering.[15,16] GO has been considered as an interesting surface support due to easy functionalization, high surface area, good thermal stability, and better dispersion in water and other organic solvents.[17,18] The strategy of functionalization on the GO sheets include two approaches such as (a) covalent functionalization of the intercalant by the ring opening of epoxides or chemical conjugation on the secondary —OH moieties or coupling on the terminal acid moieties[19–22] and (b) noncovalent interactions on the surface of GO through van der Waals interactions using aromatic substrates.[23–26] Spyrou et al. have demonstrated the intercalation of organic polycyclic aromatic amines in the GO planes and proved that its interaction with GO differs with the size of the intercalants.[27] Teo et al. have reported the non-covalent interaction of aminopyrene with reduced GO as a supercapacitor electrode.[28] Ajay Gupta et al. have developed an easy and efficient click method for the synthesis of flavanone-containing triazole moiety catalyzed by CuO/rGO nanocomposite.[29] The catalytic activity of GO supported copper oxide (CuO–GO) has been investigated in click synthesis of 1,2,3-triazole derivatives under green reaction conditions by Reddy et al.[30] Zhao et al. studied the immobilized copper (salen) complex on GO for the epoxidation of olefins.[31] We have proved in our previous work, the enhanced interlayer *d*-spacing of GO sheets due to covalent intercalation of phthalimide protected DETA.[32] Epoxidation of olefins was performed by Masteri-Farahani et al. using peroxophosphotungstate anion in the GO basal planes.[33] Gorji et al. reported the synthesis of Cu(II) Schiff base complex immobilized on GO/α-$Fe_2O_3$ as heterogeneous catalyst for the three-component synthesis of 2-Amino-4H-Chromenes derivatives.[34] Therefore, it is of our interest to prepare the versatile GO nanocomposites through the intercalation of high stable $Cu^{II}$ complexes in the GO basal planes and to demonstrate its catalytic activity towards the click reaction. In this work, we report the noncovalent interaction of $Cu^{II}$ complexes of bipyridine and phenanthroline Ligands on GO nanocomposites as efficient catalysts for click reaction.

## 2 | EXPERIMENTAL METHODS

### 2.1 | Synthesis of copper(II) complexes (C1 and C2)

The copper(II) complexes of bipyridine and phenanthroline were prepared by the modified method.[35,36] To the solution of the ligands, bipyridine, or phenanthroline (1 equiv.) in 30 ml of methanol, copper(II) perchlorate hexahydrate (0.5 equiv.) in 20 ml of methanol was added dropwise over the period of 1 h under argon atmosphere. The resulting solution was refluxed for overnight. Then, the reaction mixture was cooled, and the solvent was removed by rotary evaporator. The blue colored solid was washed with diethyl ether to get the respective powdered Cu(II) complexes and stored in vacuum desiccators.

### 2.2 | Intercalation of ($Cu^{II}$ $(bpy)_2$) C1 and ($Cu^{II}$ $(phen)_2$) C2 onto the GO planes

GO was synthesized by the reported method.[37] The intercalation of $Cu^{II}$ complexes into the GO sheets was performed by the dropwise addition of C1 or C2 to the well-dispersed solution of GO under high dilution condition. In the typical procedure, GO (1 g) was dispersed in 200 ml of distilled water and sonicated for one hour. To the dispersed GO solution, corresponding copper(II) complex C1 or C2 (1 g) in 50 ml of ethanol was added dropwise and stirred for about 12 h. Upon the intercalation, the brown dispersed solution was changed to black color. The black solid was centrifuged and washed with water and ethanol to remove the excess of $Cu^{II}$ complexes. Diethyl ether was added to remove all the residual solvents and dried at RT to isolate the free-flow black solid.

### 2.3 | General procedure for CuAAC reaction

In a round bottom flask fitted with stopper, phenyl acetylene (1.0 mmol), an organic azide (1.0 mmol), GO-C1 or GO-C2 (50 mg) were added in 2 ml of *t*-butanol followed by the addition of sodium ascorbate (10 mg) dissolved in 3 ml of water. The reaction mixture was stirred at room temperature for about 60 min. The GO-based catalyst was filtered and the resulting reaction mixture was diluted with ethyl acetate (50 ml) and water (5 ml) to get biphasic layer. The organic layer was separated and dried over anhydrous sodium sulfate and concentrated under reduced pressure. The crude product was purified using silica gel column chromatography (Eluents: Hexane-Ethyl acetate, 6:4 *v/v*) to isolate the corresponding 1,4-disubstitued-1,2,3-triazole (1c-5c) in good yield.

### 2.4 | Characterization

The absorbance was recorded at 200–800 nm using Perkin Elmer Lambda 35 UV–Vis spectrophotometer.

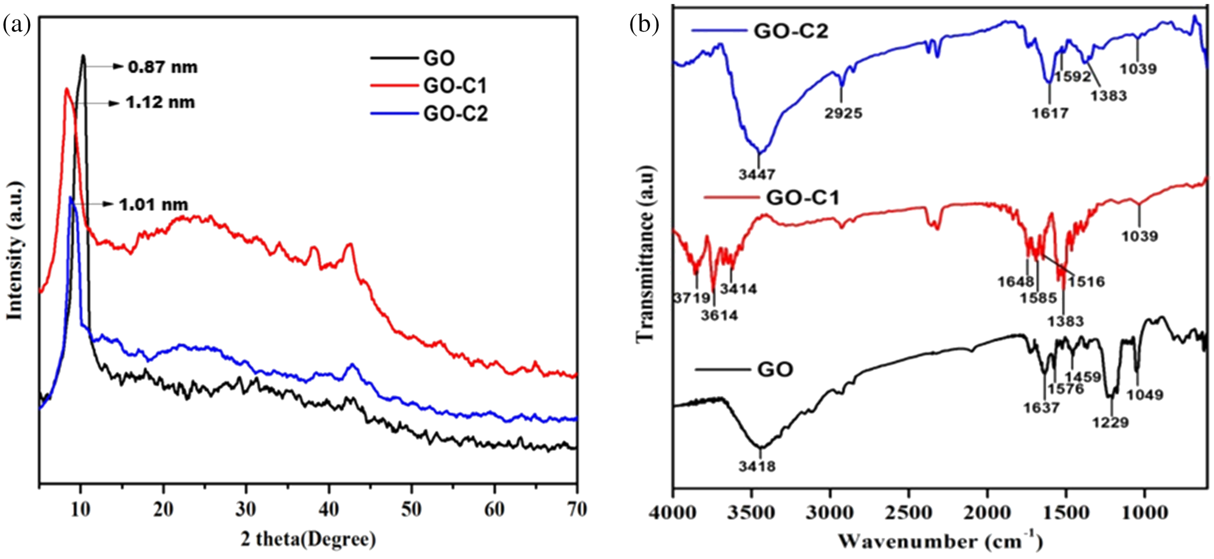

**FIGURE 1** (a) Powder X-ray diffraction (XRD) spectra of graphene oxide (GO), GO-C1, and GO-C2; (b) Fourier-transform infrared spectroscopy (FT-IR) spectra of GO, GO-C1, and GO-C2

Fourier-transform infrared spectroscopy (FT-IR) analysis was carried out with the spectral range of 400–4,000 cm$^{-1}$ using IR-Prestise-21 Shimadzu instrument. The crystalline structure of the GO, GO-C1, and GO-C2 nanocomposites were studied using X-ray diffraction (XRD) technique. The XRD patterns were recorded on a Shimadzu XRD-6000 Powder X-Ray diffractometer at 40 kV voltages and 30 mA current. All the spectra were acquired at a pressure using ultra high vacuum with Al Kα excitation at 250 W. Scanning electron microscope (SEM) images were measured by Hitachi S4800 field emission SEM system. X-ray photoelectron spectroscopic (XPS) analysis was carried out in axis ultra multitechnique XPS. All the spectra were acquired at a pressure using ultra high vacuum with Al Kα excitation at 250 W. Raman spectra were recorded on a Horiba-Jobin Raman spectrometer with a 514 nm laser power. Thermogravimetric analysis (TGA) measurements were carried out under a $N_2$ atmosphere using NETZSCH STA 449 F3 Jupiter. Transmission electron microscopic (TEM) images were recorded using a JEOL JEM-2100 transmission electron microscope operating at 200 kV. The loading content of copper of the GO-C1 and GO-C2 was determined by inductively coupled plasma optical emission spectroscopy (Vista-MPX, Perkin Elmer ICPOES, Model 5300 DV). $^{1}$H and $^{13}$C-NMR spectra of click products were recorded with a Bruker Avance III HD Nanobay 400 MHz FT-NMR Spectrometer. Mass spectrum of the Cu(II) complexes and triazole compounds were recorded in Agilent mass spectrometer LCMS-1260 INFINITY II under nitrogen atmosphere. The azides were prepared from the corresponding halides treated with sodium azide in dry acetone.[38]

## 3 | RESULTS AND DISCUSSION

The powder XRD patterns of GO-C1 and GO-C2 nanomaterials show the diffraction peaks at 2θ value of 8.77° and 9.06° with the enhanced interlayer *d*-spacing of 1.12 and 1.01 nm, respectively, due to the intercalation of C1 and C2 complexes into the basal planes of GO (Figure 1a). In addition, the notable diffraction peaks at 37.90° and 39.50° correspond to (111) plane of monoclinic CuO (JCPDS 80-1917) and at 42.40°, 49.90° and 42.60°, 48.00° were indexed to (111) and (200) planes of metallic Cu particles (JCPDS 04-0836) exist in the GO-C1 and GO-C2 nanocomposites, respectively.[39–41] The as-prepared composites were also characterized by FT-IR, XPS, Raman, and UV spectroscopic techniques. FT-IR spectra of GO-C1 and GO-C2 material (Figure 1b) show the characteristic peaks at 3,614, 3,414 cm$^{-1}$ and 3,654, 3,447 cm$^{-1}$ correspond to $NH_{str}$ and $OH_{str}$ vibrations, respectively. The peaks at 1,648, 1,617 cm$^{-1}$ and 1,516, 1,592 cm$^{-1}$ correspond to C═O and $C═C_{str}$ vibrations of GO-C1 and GO-C2 respectively. The peak at 1383 and 1,039 cm$^{-1}$ corresponds to C—N (amine) stretching vibrations and $C—O—C_{str}$ vibrations of GO-C1 and GO-C2, respectively.

XPS analysis was performed to understand the effect of intercalation and evaluate the oxidation state of copper metal, binding energies, and elemental composition of as-prepared materials. In our previous work, we have reported the XPS spectra of the GO which shows the two characteristic peaks at 284 and 532 eV corresponding to the C1s and O1s binding energies, respectively.[37] The XPS survey spectrum of GO-C1 and GO-C2 (Figure 2a) shows the significant binding energy at 399–405 eV for

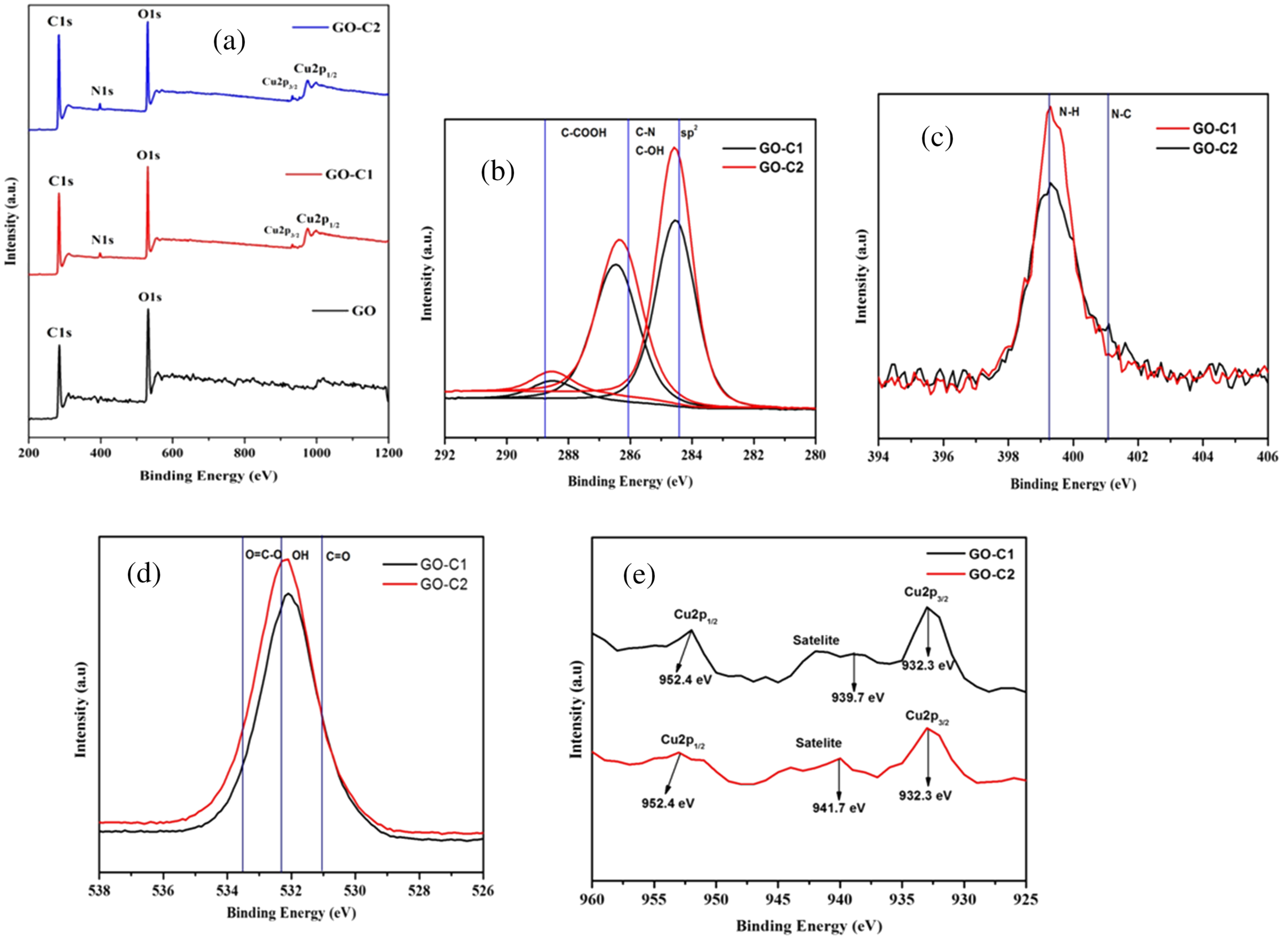

**FIGURE 2** (a) X-ray photoelectron spectroscopy (XPS) survey spectrum of graphene oxide (GO), GO-C1, and GO-C2; (b) Deconvoluted C1s of GO-C1 and GO-C2; (c) Deconvoluted N1s of GO-C1 and GO-C2; (d) Deconvoluted O1s of GO-C1 and GO-C2; (e) Core level spectrum of Cu 2p of GO-C1 and GO-C2

N1s and 931–952 eV for core-level spectrum of Cu 2p, which confirms the intercalation of Cu(II) tetraaza complexes in between the GO planes. The deconvoluted XPS spectra of C1s spectra (Figure 2b) of GO-C1 and GO-C2 shows the deconvoluted bands at 284.5, 286.4, and 288.4 eV which correspond to C—C/C═C, C—OH and COOH, respectively. The N1s spectra (Figure 2c) of GO-C1 and GO-C2 show two deconvoluted bands at 399.3 and 401.3 eV were assigned to the N—H of amine and protonated N-atoms, respectively. The O1s spectra (Figure 2d) shows two deconvoluted bands at 531 and 532.5 eV correspond to —OH of primary alcohol and C═O of carboxylic acid, respectively. Moreover, the binding energy peaks at 952.4 and 932.3 eV correspond to the spin-orbit splitting components of Cu $2p_{1/2}$ and Cu $2p_{3/2}$ of $Cu^+$ and $Cu^{2+}$ species of GO-C1 and GO-C2 (Figure 2e). The further satellite peaks for Cu $2p_{3/2}$ and Cu $2p_{1/2}$ were observed at 944 and 962 eV that indicates the +2 oxidation state of copper metal in the GO-C1and GO-C2 composite.[42–44]

The Raman spectra of GO shows two bands at 1,349 and 1,592 $cm^{-1}$ corresponds to the D and G bands respectively[32] and in the case of as-prepared catalysts also show two bands each at 1,322.78 and 1,520.28 $cm^{-1}$ for GO-C1 and 1,326.54 and 1,516.73 $cm^{-1}$ for GO-C2, which are assigned to D band and G band, respectively (Figure 3a). The $I_D/I_G$ value is found to be 0.87 for GO-C1 and 0.88 for GO-C2 composite.[45,46] The UV absorbance of GO-C1 shows the shifted peaks at 248 and 307 nm were assigned to π-π* transitions of C═C, n-π* transitions of C═N bonds, respectively. In the case of GO-C2 composite, the absorbance bands at 206, 229, 265, and 300 nm correspond to π-π* transitions of C═C, π-π* transitions in $Cu^{II}$ tetraaza complex and n-π* transitions of C═N, respectively (Figure 3b).[47] The GO-C1 and GO-C2 nanocomposites show the redshift indicates the π electrons interaction with GO and $Cu^{II}$ complexes. The thermal stability of intercalated GO-C1 and GO-C2 nanocomposites were investigated by TGA analysis and shown in Figure 3c. These composites show the initial

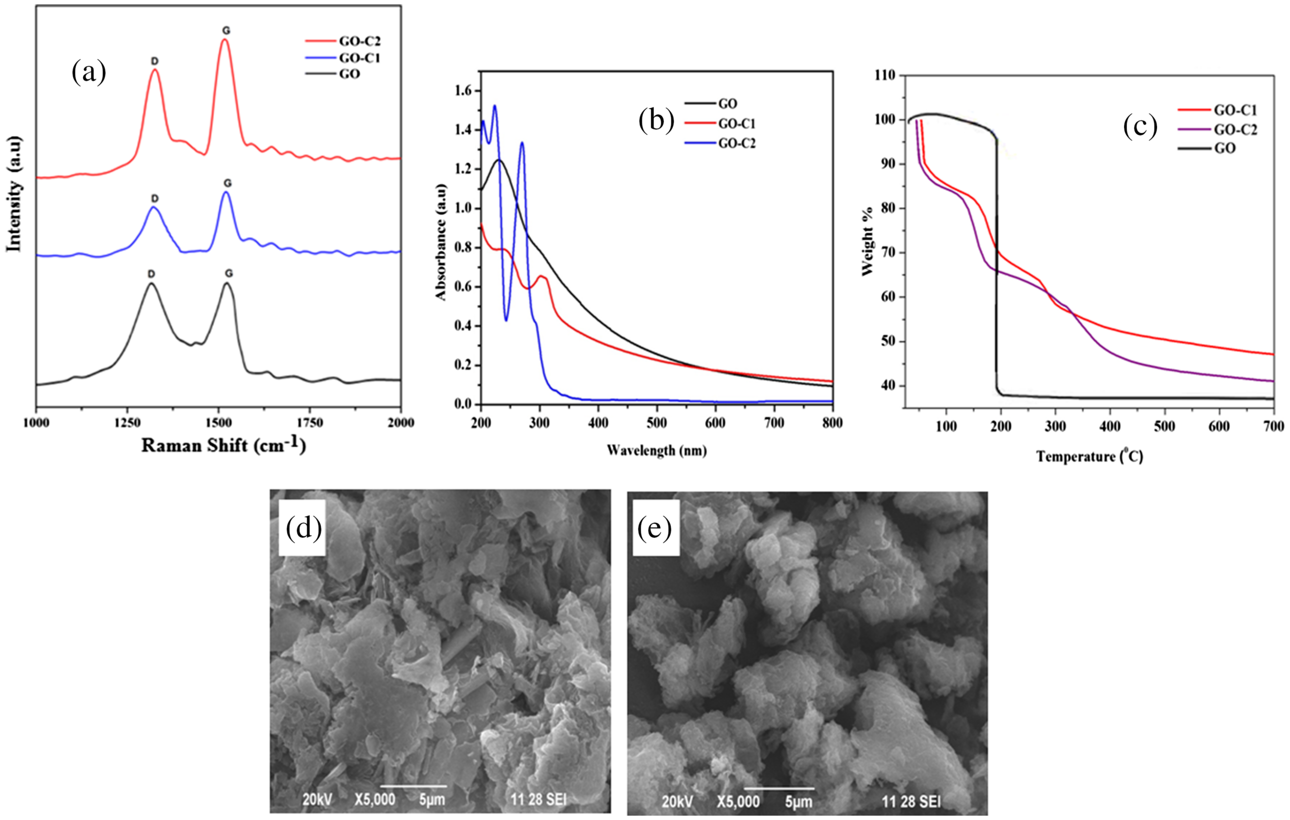

**FIGURE 3** (a) Raman spectrum; (b) UV Spectrum; (c) thermogravimetric analysis (TGA) analysis of graphene oxide (GO), GO-C1, and GO-C2; (d) scanning electron microscope (SEM) image of GO-C1; (e) SEM image of GO-C2

weight loss of around 21% at 100°C which attributes the removal of intercalated water. The significant weight loss was shown at 150°C–190°C (17%) attributed to the thermal decomposition of unutilized oxygen-containing functionalities. The maximum weight loss observed in the temperature was from 350°C to 700°C due to the slow decomposition of intercalated $Cu^{II}$ tetraaza complexes.[48,49]

The SEM and high-resolution transmission electron microscopy (HR-TEM) analysis were performed to investigate the microstructure and morphology of GO upon the functionalization of C1 and C2. The SEM images of GO-C1 and GO-C2 were shown in Figure 3d,e. The SEM images show the sheet-like structure with the wrinkled surface due to the intercalation whereas the GO sheets present the granulate surface textures with spherical edges.[50–52] In TEM analysis at different-magnification, GO-C1 and GO-C2 shows typical rippled and crumpled morphology in which the nanosheet contains many wrinkles throughout the surface respectively as seen in SEM images (Figure 4a,e). Such characteristic surface wrinkling would be an important advantage for applications in catalytic reactions, due to the higher accessibility of the catalytic sites. While high resolution TEM images of GO-C1 and GO-C2 show the significant irregular stacked layered structure and dark zones even at wrinkled edges which clearly shows that the layered structure associated with the dispersed C1 and C2 on the surface as depicted in Figure 4b,c,f,g. The appearance of the selected area electron diffraction (SAED) pattern images of GO-C1 and GO-C2 indicates multilayered crystalline structure (Figure 4d,h). A typical sharp, polycrystalline ring pattern was observed. The first ring corresponds to the (1100) plane and the second ring attributed to the (1120) of GO basal planes.[53] The unequal intensity of the diffraction spots in the SAED pattern might be due to the adsorption of intercalants (C1 or C2) on the surface of GO. The quantitative analysis of the copper content in the catalyst was determined by inductively coupled plasma optical emission spectroscopy (ICP-OES), and the copper content of 3.40% and 3.22% (*w/w*) were detected for GO-C1 and GO-C2, respectively (Table S2).

The existing Van der Waals interaction of the copper complexes (C1 and C2) on the GO basal planes in the layered structures facilitates the heterogeneous catalyst to immobilize on the GO planes due to the availability of the surface functionalities. The significant catalytic activity was not only due to the good dispersion of GO-C1 and

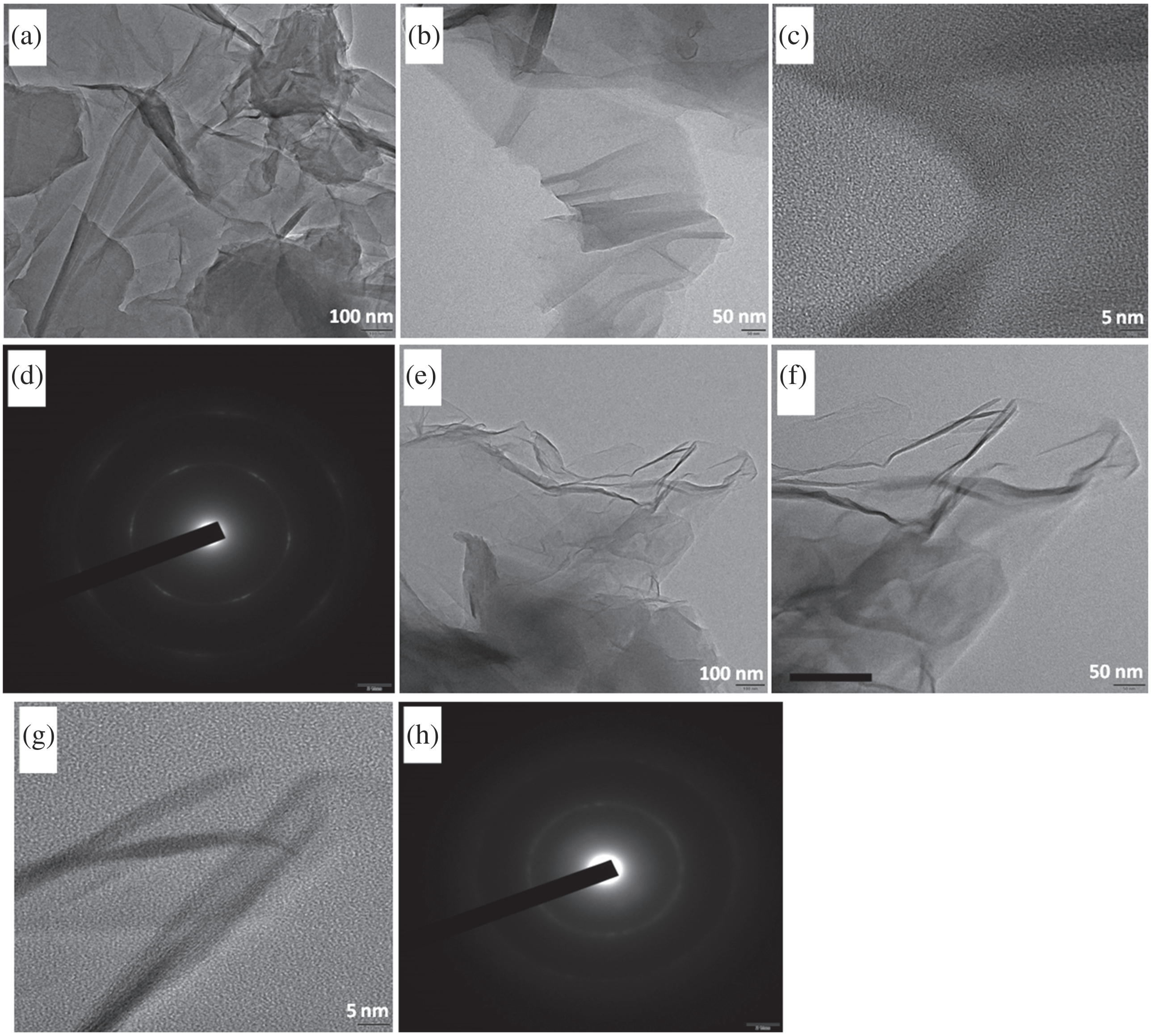

**FIGURE 4** Transmission electron microscopic (TEM) image and a typical selected area electron diffraction (SAED) pattern of the graphene oxide (GO)-C1 (a–d) and GO-C2 (e–h)

GO-C2 nanosheets in the heterogeneous mixture but also facilitate the mass transfer of organic precursors into products under the reaction condition.

## 3.1 | Click reaction using GO-C1 and GO-C2 nanocomposites

It is of our interest to explore the catalytic properties of GO-C1 and GO-C2 composites for $Cu^{II}$AAC alkyne-azide coupling reaction in green solvents.[54–56] The typical click reaction of phenyl acetylene with benzyl azide was performed by the catalysts (50 mg) and sodium ascorbate (10 mg) at RT using *t*-butanol/$H_2O$ as a solvent. The desired product, 1,4-disubstituted-1,2,3 triazole was isolated as 91% and 88% yield using GO-C1 and GO-C2 catalysts, respectively (Scheme 1).

To demonstrate the scope of the click protocol using GO-C1, we have chosen the series of azides containing an electron-donating and electron-withdrawing group to perform click reaction with phenyl acetylene under optimized conditions to achieve their corresponding 1,4-disubstituted-1,2,3-triazoles and the results are tabulated in Table 1. It is noteworthy to report that the intercalated nanocomposites are convenient, reproducible, and reusable as click catalysts for alkyl and aryl azide substrates.

The high catalytic activity of GO-C1 is attributed due to the hydrophilic nature of GO surface and also due to the "Breslow effect."[57,58] According to the "Breslow

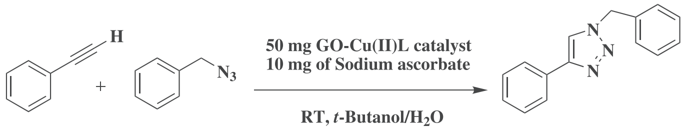

**1a**

**SCHEME 1** Optimization of the synthesis of triazole using GO-Cu(II)L catalyst

**TABLE 1** Table of optimization of GO-Cu(II)L catalyst with time and isolated yield

| GO-Cu(II)L Catalyst | Time (min) | Yield (%) |
|---|---|---|
| GO-C1 | 60 | 91 |
| GO-C2 | 80 | 88 |

Abbreviation: GO, graphene oxide.

effect” during the reaction, the well dispersed functionalized GO catalyst (GO-C1 or GO-C2) in organic/aqueous solvent mixture facilitates the cycloaddition of phenyl acetylene and aryl azide using copper complex (C1 or C2) supported on the surface of GO as an active sites within the nanocomposites and thereby increasing the yields of 1,2,3-triazoles. The addition of

**TABLE 2** Various azides utilized and the respective triazole products with time and isolated yield

| Entry | R-$N_3$ (1b-5b) | Time (min) | Isolated product (1c-5c) | Yield (%) | Yield (g) |
|---|---|---|---|---|---|
| **1** | 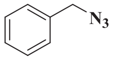 | 60 | 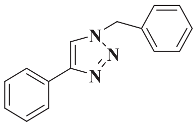 | 91 | 0.213 |
| **2** | 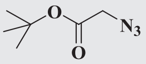 | 70 | 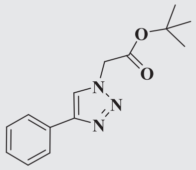 | 89 | 0.231 |
| **3** | 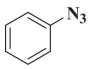 | 65 | 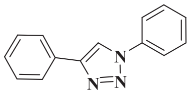 | 83 | 0.183 |
| **4** | 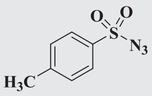 | 75 | 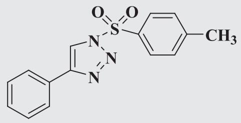 | 80 | 0.239 |
| **5** | 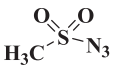 | 80 | 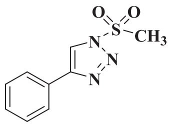 | 81 | 0.181 |

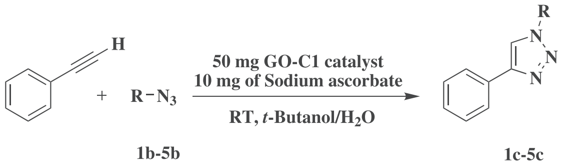

**SCHEME 2** General scheme of the $Cu^{II}$AAC reaction using GO-C1

catalytic amount of the sodium ascorbate during the reaction involves in the initiation of the reduction of Cu(II)L supported on the GO, which promotes product formation by accelerating the electron transfer process. Hence, the heterogeneous GO support is required for the cycloaddition of various acetylene-azide organic precursors resulting in high yields with enhanced catalytic activity of GO-C1 catalyst (Table 2) (Scheme 2).

## 3.2 | Reusability study of GO-C1

After completion of the click reaction of first cycle, the heterogeneous catalyst GO-C1 was filtered and washed with ethyl acetate followed by acetone and water thrice and was rinsed with diethyl ether in the end. The solid GO-C1 catalyst was dried at room temperature for about 12 h and used for the next two batches of click reaction of phenyl acetylene and benzyl azide to get the triazole product in considerable moderate yield (Table 3).

## 3.3 | Optimization of reaction conditions of click reaction catalyzed by GO-C1

The effect of catalyst dosage and solvent were studied in optimizing the reaction conditions of click reaction of phenyl acetylene and benzyl azide catalyzed by GO-C1. From the below table, it was inferred that 50 mg of GO-C1 was the most effective catalytic amount and the best yield was obtained in $t$-Butanol/$H_2O$ (2:3 $v/v$) solvent mixture for the CuAAC reaction (Table 4).

**TABLE 3** Recyclability of GO-C1 nanocomposite materials and its yield

| Entry | GO-C1 catalyst[a] | Yield (%)[b] |
|---|---|---|
| 1 | Click reaction | 91 |
| 2 | Recycle 1 | 69 |
| 3 | Recycle 2 | 60 |

[a]Reaction conditions: Phenyl acetylene (1 mmol), Benzyl azide (1 mmol) GO-C1 catalyst (50 mg) and Sodium ascorbate (10 mg) were reacted in 2:3 $t$-butanol/$H_2O$ at RT.
[b]Isolated yield of 1-benzyl-4-phenyl-1*H*-1,2,3-triazole.

**TABLE 4** Various solvent effects for the isolation of better yields

| Entry | GO-C1 catalyst (mg)[a] | Solvent | Yield (%)[b] |
|---|---|---|---|
| 1 | - | $t$-Butanol/$H_2O$ (2:3 $v/v$) | 0 |
| 2 | 10 | $t$-Butanol/$H_2O$ (2:3 $v/v$) | 50 |
| 3 | 25 | $t$-Butanol/$H_2O$ (2:3 $v/v$) | 76 |
| 4 | 50 | $t$-Butanol/$H_2O$ (2:3 $v/v$) | 91 |
| 5 | 50 | $t$-Butanol | 80 |
| 6 | 50 | Ethanol | 67 |
| 7 | 50 | $CH_3CN$ | 77 |
| 8 | 50 | $H_2O$ | 64 |
| 9 | 50 | DMSO | 51 |

[a]Reaction conditions: Phenyl acetylene (1 mmol), benzyl azide (1 mmol), and sodium ascorbate (10 mg) were reacted at RT.
[b]Isolated yield of 1-benzyl-4-phenyl-1*H*-1,2,3-triazole.

## 4 | CONCLUSION

The new class of GO composite materials was successfully prepared by the intercalation of Cu(II) tetraaza complexes into the GO layers and thereby the enhanced interlayer *d*-spacing was achieved. The noncovalent intercalation of $Cu^{II}$ complexes on the GO sheets was confirmed by spectroscopic and microscopic analysis. The XPS survey spectra confirms the intercalation of C1 and C2 in between the GO planes by showing significant binding energy of 399–405 eV for N1s and 932.3 eV for Cu. These composites were used as efficient, green, click catalysts for alkyne-azide cycloaddition ($Cu^{II}$AAC) reaction and could facilitate the electron transfer rate by stabilizing Cu(I) intermediates in the catalytic cycle in the click mechanism. The as-prepared click catalysts could be used for the development of click products from proteins, peptides and amino acids in green solvents.

## ACKNOWLEDGMENTS

The authors sincerely thank UGC DAE Consortium Scientific Research, IGCAR-Kalpakkam, for the grant (no.: CSR/Acctts/2016-17/1347) and Department of Science and Technology, DST-DPRP division (no.: VI-D&P/562/2016-17/TDT(C)) for their research grant to carry out this research.

## AUTHOR CONTRIBUTIONS

**Angel Green Samuel:** Formal analysis; investigation; visualization. **Karthikeyan Nagarajan:** Formal analysis; software; validation; visualization. **Karthick Cidhuraj:** Formal analysis; software; validation. **Bhalerao Gopal:** Formal analysis; methodology; resources; validation. **Sujay Chakravarty:** Formal analysis; methodology; resources; validation. **Varadharajaperumal Selvaraj:** Formal analysis; methodology; software; validation. **Emmanuvel Lourdusamy:** Formal analysis; methodology; software; validation. **JEBASINGH Bhagavathsingh:** Conceptualization; formal analysis; investigation; methodology; project administration; resources; software; supervision; validation.

## CONFLICT OF INTEREST

Authors declare no conflict of interest.

## ORCID

*Jebasingh Bhagavathsingh* https://orcid.org/0000-0003-3405-6208

## REFERENCES

[1] D. Chen, H. Feng, J. Li, *Chem. Rev.* **2012**, *112*, 6027.
[2] K. P. Loh, Q. Bao, G. Eda, M. Chhowalla, *Nat. Chem.* **2010**, *2*, 1015.
[3] Y. Deng, Y. Li, J. Dai, M. Lang, X. Huang, *Polymer Sci., Part a: Polymer Chem* **2011**, *49*, 4747.
[4] A. K. Geim, K. S. Novoselov, *World Scientific.* **2009**, 11.
[5] G. Zhao, X. Li, M. Huang, Z. Zhen, Y. Zhong, Q. Chen, X. Zhao, Y. He, R. Hu, T. Yang, R. Zhang, C. Li, J. Kong, J. Xu, R. S. Ruoff, H. Zhu, *Chem. Soc. Rev.* **2017**, *46*, 4417.
[6] M. Coros, F. Pogacean, L. Magerusan, C. Socaci, S. Pruneanu, *Frontiers Mater. Sci.* **2019**, *13*, 23.
[7] H. Wang, M. Pumera, *Chem. Rev.* **2015**, *115*, 8704.
[8] A. H. Castro Neto, F. Guinea, N. M. R. Peres, K. S. Novoselov, A. K. Geim, *Rev. Mod. Phys.* **2009**, *81*, 109.
[9] C. N. Lau, W. Bao, J. Velasco, *Mater. Today* **2012**, *15*, 238.
[10] M. Pumera, *Chem. Rev.* **2009**, *9*, 211.
[11] S. Park, R. S. Ruoff, *Nature Nanotechnol.* **2009**, *4*, 217.
[12] D. R. Dreyer, S. Park, C. W. Bielawski, R. S. Ruoff, *Chem. Soc. Rev.* **2010**, *39*, 228.
[13] M. Xu, J. Zhu, F. Wang, Y. Xiong, Y. Wu, Q. Wang, J. Weng, Z. Zhang, W. Chen, S. Liu, *ACS Nano* **2016**, *10*, 3267.
[14] S. Presolski, M. Pumera, *Angew. Chem., Int. Ed.* **2018**, *57*, 16713.
[15] S. K. Sahoo, G. Hota, *ACS Appl. Nano Mater.* **2019**, *2*, 983.
[16] M. Batzill, *Surf. Sci. Rep.* **2012**, *67*, 83.
[17] R. R. Amirov, J. Shayimova, Z. Nasirova, A. M. Dimiev, *Carbon* **2017**, *116*, 356.
[18] R. Rozada, J. I. Paredes, S. Villar-Rodil, A. Martinez-Alonso, J. M. D. Tascon, *Nano Res.* **2013**, *6*, 216.
[19] C. C. Caliman, A. F. Mesquita, D. F. Cipriano, J. C. C. Freitas, A. A. C. Cotta, W. A. A. Macedo, A. O. Porto, *RSC Adv.* **2018**, *8*, 6136.
[20] R. K. Singh, R. Kumar, D. P. Singh, *RSC Adv.* **2016**, *6*, 64993.
[21] A. M. Shanmugharaj, J. H. Yoon, W. J. Yang, S. H. Ryu, *J. Coll. Inter. Sci.* **2013**, *401*, 148.
[22] M. Pumera, C. H. A. Wong, *Chem. Soc. Rev.* **2013**, *42*, 5987.
[23] R. Bendi, T. Imae, *RSC Adv.* **2013**, *3*, 16279.
[24] H. Zhang, H. Zhang, T. Kuila, N. H. Kim, D. S. Yu, J. H. Lee, *Carbon* **2014**, *69*, 66.
[25] P. Khanra, T. Kuila, S. H. Bae, N. H. Kim, J. H. Lee, *J. Mater. Chem.* **2012**, *22*, 24403.
[26] D. Parviz, S. Das, H. S. T. Ahmed, F. Irin, S. Bhattacharia, M. J. Green, *ACS Nano* **2012**, *6*, 8857.
[27] K. Spyrou, M. Calvaresi, E. K. Diamanti, T. Tsoufis, D. Gournis, P. Rudolf, F. Zerbetto, *Adv. Funct. Mater.* **2014**, *25*, 263.
[28] E. Y. L. Teo, H. N. Lim, R. Jose, K. F. Chong, *RSC Adv.* **2015**, *5*, 38111.
[29] A. Gupta, R. Jamatia, R. A. Patil, Y. Ma, A. K. Pal, *ACS Omega* **2018**, *3*, 7288.
[30] V. H. Reddy, Y. V. R. Reddy, B. Sridhar, B. V. S. Reddy, *Adv. Synth. Catal.* **2016**, *358*, 1088.
[31] Q. Zhao, C. Bai, W. Zhang, Y. Li, G. Zhang, F. Zhang, X. Fan, *Ind. Engg. Chem. Res.* **2014**, *53*, 4232.
[32] P. Ramesh, B. Jebasingh, *Mater. Chem. Phy.* **2019**, *222*, 45.
[33] M. Masteri-Farahani, M. Modarres, *Appl. Organometal. Chem.* **2017**, e4142.
[34] F. M. Gorji, N. Monadi, *Synth. Met.* **2019**, *258*, 116199.
[35] T. Hirohama, Y. Kuranuki, E. Ebina, T. Sugizaki, H. Arii, M. Chikira, P. Tamil Selvi, M. Palaniandavar, *J. Inorg. Biochem.* **2005**, *99*, 1205.
[36] J. L. Gray, D. L. Gerlach, E. T. Papish, *Acta Cryst.* **2017**, *E73*, 31.
[37] P. Ramesh, B. Jebasingh, *Mater. Lett.* **2017**, *193*, 305.
[38] Chemistry of Halides, Pseudo-Halides and Azides, Part 2, in, (Ed: S. Patai), John Wiley & Sons Ltd, Chichester **1995**.
[39] S. Chen, J. Zhu, X. Wu, Q. Han, X. Wang, *ACS Nano* **2010**, *4*, 2822.
[40] H. Zhang, K. Wang, X. Zhang, H. Lin, X. Sun, C. Li, Y. Ma, *J. Mater. Chem. A* **2015**, *3*, 11277.
[41] T. Tsoufis, F. Katsaros, Z. Sideratou, B. J. Kooi, M. A. Karakassides, A. Siozios, *Chem. – Eur. J.* **2014**, *20*, 8129.
[42] A. Kumar, S. Layek, B. Agrahari, S. Kujur, D. D. Pathak, *Chem. Select* **2019**, *4*, 1337.
[43] X. Zhang, D. Zhang, Y. Chen, X. Sun, Y. Ma, *Chineese Sci. Bull.* **2012**, *57*, 3045.
[44] U. Saha, R. Jaiswal, T. H. Goswami, *Electrochim. Acta* **2016**, *196*, 386.
[45] K. N. Kudin, B. Ozbas, H. C. Schniepp, R. K. Prud'homme, I. A. Aksay, R. Car, *Nano Lett.* **2001**, *8*, 36.
[46] J. Park, M. Yan, *Acc. Chem. Res.* **2013**, *46*, 181.
[47] S. Bae, H. Kim, Y. Lee, X. Xu, J. Park, Y. Zheng, J. Balakrishnan, T. Lei, H. R. Kim, Y. I. Song, Y. Kim, K. S. Kim, B. Özyilmaz, J. Ahn, B. H. Hong, S. Iijima, *Nat. Nanotechnol.* **2010**, *5*, 574.
[48] F. Najafi, M. Rajabi, *Int. Nano Lett.* **2015**, *5*, 187.
[49] A. Gupta, S. K. Saha, *Nanoscale* **2012**, *4*, 6562.
[50] T. Kuila, S. Bose, P. Khara, A. K. Mishra, N. H. Kim, J. H. Lee, *Carbon* **2012**, *50*, 914.

[51] K. Zhang, L. Mao, L. L. Zhang, H. S. O. Chan, X. S. Zhao, J. Wu, *J. Mater. Chem.* **2011**, *21*, 7302.

[52] D. Chen, L. Li, L. Guo, *Nanotechnology* **2011**, *22*, 325601.

[53] M. Jana, P. Khanra, N. C. Murmu, P. Samanta, J. H. Lee, T. Kuila, *Mater. Chem. Phys.* **2016**, *16*, 7618.

[54] H. C. Kolb, M. G. Finn, K. B. Sharpless, *Angew. Chem., Int. Ed.* **2001**, *40*, 2004.

[55] P. Thirumurugan, D. Matosiuk, K. Jozwiak, *Chem. Rev.* **2013**, *113*, 4905.

[56] H. Zhao, Q. Zhu, Y. Gao, P. Zhai, D. Ma, *Appl. Catal. A* **2013**, *456*, 233.

[57] R. Breslow, *Acc. Chem. Res.* **1992**, *24*, 159.

[58] C. B. Putta, V. Sharavath, S. Sarkar, S. Ghosh, *RSC Adv.* **2015**, *5*, 6652.

## SUPPORTING INFORMATION

Additional supporting information may be found online in the Supporting Information section at the end of this article.

**How to cite this article:** Samuel AG, Nagarajan K, Cidhuraj K, et al. Copper(II) complex intercalated graphene oxide nanocomposites as versatile, reusable catalysts for click reaction. *Appl Organomet Chem*. 2020;e6017. https://doi.org/10.1002/aoc.6017